International Journal of Solids and Structures 257 (2022) 111371

Contents lists available at ScienceDirect

International Journal of Solids and Structures

journal homepage: www.elsevier.com/locate/ijsolstr

On the dissipation at a shock wave in an elastic bar

Prashant K. Purohit [a], Rohan Abeyaratne [b,*]

[a] Department of Mechanical Engineering and Applied Mechanics, University of Pennsylvania, Philadelphia, PA, 19104, USA
[b] Department of Mechanical Engineering, Massachusetts Institute of Technology, Cambridge, MA, 02139, USA

ARTICLE INFO

Keywords:
Shock wave
Dissipation
Dispersion
Elastic bar
Discrete chain
Dispersive shock wave
Oscillations

ABSTRACT

This paper aims to relate the energy dissipated at a shock wave in a nonlinearly elastic bar to the energy in the oscillations in two related dissipationless, dispersive systems. Three, one-dimensional, dynamic impact problems are studied: Problem 1 concerns a nonlinearly elastic bar, Problem 2 a discrete chain of particles, and Problem 3 a continuum with a strain gradient term in the constitutive relation. In the impact problem considered, the free boundary of each initially quiescent body is subjected to a sudden velocity, that is then held constant for all subsequent time. There is energy dissipation at the shock in Problem 1, but Problems 2 and 3 are conservative. Problem 1 is solved analytically, Problem 2 numerically, and an approximate solution to Problem 3 is constructed analytically. The rate of increase of the oscillatory energy in Problems 2 and 3 are calculated and compared with the dissipation rate at the shock in Problem 1. The results indicate that the former is a good qualitative measure of the latter. The quantitative agreement is satisfactory at larger impact speeds but less so at smaller speeds, some possible reasons for which are discussed.

1. Introduction

Dissipation in an elastic body sounds like a contradiction, since we often think of "elastic" as being synonymous with "dissipationless". However, if an elastic body, even a hyperelastic body, involves a moving singularity such as a shock wave,[1] there is a loss of energy at the singularity. This is usually attributed to a deficiency in the elastic model, at least when it comes to modeling such a feature. This leads to "regularization" of the theory, which entails accounting for other physical effects.

For example a dissipative regularization involves adding, say, a viscous term to the elastic constitutive relation, and this causes the sharp elastic shock fronts to turn into narrow zones in which the fields vary continuously (but rapidly). However, if one wants to examine the dissipation in the elastic body, as we do, one should not augment the model with additional sources of dissipation. Therefore we shall not pursue dissipative regularizations of the elasticity problem.

On the other hand a dissipationless, dispersive regularization would involve adding, say, a conservative strain-gradient term to the elastic constitutive equation. The shock wave in the elastic body is now replaced by a dispersive wave packet. It is usually claimed that the energy in the oscillations of the wave packet correspond to the energy dissipated at the shock wave in the elastic body. While this is certainly plausible, and even likely, we have not found an investigation of this in the literature, and that is the focus of this paper.

We consider three closely related problems. Problem 1 concerns a semi-infinite nonlinearly elastic bar. The bar is initially stress free and at rest. At time $t = 0^+$ its free boundary is given a speed V which is held constant from then on. A shock wave emerges from the loading surface $x = 0$, and propagates into the quiescent material at a constant speed. The strain γ^- and particle speed $v^- = -V$ behind the shock are constant. The problem can be readily solved analytically, and in particular, the dissipation rate calculated explicitly.

Problem 2 is a discrete counterpart of Problem 1. It involves a semi-infinite row of identical particles, with each particle interacting with its nearest neighbors through identical nonlinearly elastic springs. The force–displacement relation of a spring is related to the stress–strain relation of the continuum. This system is dissipationless. The spacing between the particles introduces a length scale into the problem, and the sudden loading causes a dispersive wave packet to propagate into the quiescent material. The strain and particle speed have different constant values on either side of this wave packet, just as in a shock wave, but the waves within it, are dispersive and the fields vary smoothly. This is a dispersive non-dissipative counterpart of a shock wave, a "dispersive shock wave" (DSW). We solve this problem numerically and calculate, in particular, the energy stored in the oscillations.

Finally, Problem 3 again concerns a continuum. It is like Problem 1, except that the constitutive relation is augmented with a linear strain-gradient term. This higher gradient term introduces a length scale. This

* Corresponding author.
E-mail addresses: purohit@seas.upenn.edu (P.K. Purohit), rohan@mit.edu (R. Abeyaratne).

[1] other examples include a propagating crack or dislocation,

https://doi.org/10.1016/j.ijsolstr.2021.111371
Received 22 July 2021; Received in revised form 15 November 2021; Accepted 17 November 2021
Available online 2 December 2021

too is a dispersive conservative system. We determine an approximate solution to this problem analytically, using a calculation motivated by Whitham's theory of modulated waves, (Whitham, 1965b,a, 1970). Here too, we calculate the energy stored in the oscillations.

The main concern of this paper is the comparison of the rates of increase of oscillatory energy in Problems 2 and 3 with the dissipation rate in Problem 1. The interested reader can find the main results in Figs. 6 and 10.

It is important to emphasize that since we want the shock wave to be the *only* source of dissipation in Problem 1, the nonlinear stress–strain relation characterizing the material is taken to be monotonic and convex. This prevents the occurrence, for example, of phase transitions which have their own dissipation. Having other sources of dissipation would only muddy the central question we want to study.

Similarly, we emphasize that we are concerned entirely with the three aforementioned *mechanical* problems. In understanding the relation between their energetics, i.e. their "energy budgets", we do not wish to bring in either temperature/thermodynamics or statistical mechanics. We want to answer our question within the framework of classical mechanics.

It is also worth remarking that each of Problems 2 and 3 is meant to be a model for Problem 1. We did not undertake Problem 2 because we wanted to numerically simulate Problem 3, or vice versa. In fact we made no attempt to numerically study Problem 3. Numerical simulation of systems involving dispersive shock waves is a rich and important subject, and there is a substantial literature on it, e.g. Fornberg and Whitham (1978), Grava and Klein (2007), Hermann (2012).

When a conservative dispersive system involves a propagating "defect" such as a dislocation or phase boundary, the energy radiated by the waves traveling away from the defect can be identified with a kinetic relation, and therefore with effective dissipation. This has been noted and explored in, for example, a Frenkel–Kontorova dislocation by Atkinson and Cabrera (1965); a propagating kink by Abeyaratne and Vedantam (1999); phase transformations by Kresse and Truskinovsky (2003) and Truskinovsky and Vainchtein (2005); dynamic fracture by Hauch and Marder (1998); and for a Peierls dislocation in two-dimensions by Sharma (2005). In our context, there is no kinetic relation associated with the motion of a shock wave, and indeed our choice of problem was dictated by this.

There is a rich literature on the dynamics of one-dimensional lattices. A few of these papers include: the celebrated Fermi–Pasta–Ulam–Tsingou (FPUT) problem where the authors investigated the transfer of energy between modes in a one-dimensional chain of particles, (Fermi et al., 1955); the closed form solution to a dynamic problem for a harmonic chain, Synge (1973) and Chin (1975); the motion of a Frenkel–Kontorova dislocation, e.g. Atkinson and Cabrera (1965); the dynamics of phase transitions, e.g. Slepyan et al. (2005), Kresse and Truskinovsky (2003), Truskinovsky and Vainchtein (2005), Puglisi and Truskinovsky (2000), Purohit and Bhattacharya (2003), Zhao and Purohit (2016); the dispersive evolution of pulses in a lattice, e.g. Giannoulis and Mielke (2006); the derivation by Aubry and Proville (2009) of Rankine–Hugoniot type jump conditions for a discrete damped nonlinear lattice; and so on.

The rigorous transition from a discrete model to a continuous one is subtle, e.g. see Giannoulis et al. (2006). Depending on the specific class of "microscopic motions" considered, the same discrete model will yield different continuum models, e.g. the KdV equation (Friesecke and Pego, 1999), the Schrödinger equation (Giannoulis and Mielke, 2004), and of course the equations of classical elasticity.

There is likewise a vast literature on the dynamics of dispersive continuous systems. A subset of these are concerned with the motion of dispersive shock waves (DSWs) according to modulation theory. This body of work stemmed from the seminal ideas of Whitham (1965b,a, 1970) that have since been advanced by other researchers and used to study DSWs in compressible fluids, Bose–Einstein condensates, shallow water etc.; e.g. see the review article by El and Hoefer (2016), the dissertation by Nguyen (1987), the book by Kamchatnov (2000) and the references therein. Rigorous analyses include the work of Lax and Levermore (1983a,b,c), Gurevich and Pitaevskii (1973, 1974) and Venakides (1985). In a recent paper Gavrilyuk et al. (2020) explore shock-like fronts in dispersive systems. The simpler DSW fitting method is described in a recent paper by Nguyen and Smyth (2021). The motion of DSWs in discrete particle chains has been explored by, e.g., Dreyer and Hermann (2008); and the equations of continuum thermomechanics (except the entropy *inequality*) have been derived from a discrete particle chain using modulation theory by Dreyer et al. (2005).

The analytical approximation that we carry out in Problem 3 was motivated by the aforementioned literature on modulation theory. However, our analysis is not an exact application of this theory and involves a, physically motivated but mathematically ad hoc, assumption as we shall make clear in Section 4.2.1.

The organization of this paper is straightforward. Section 2 is devoted to Problem 1 (the elastic bar), Section 3 to Problem 2 (the discrete particle chain), and Section 4 to Problem 3 (the dispersive continuum model with strain-gradient effects). We derive an explicit relation (66) between the states γ^-, v^- behind the DSW and the state γ^+, v^+ ahead of it. It is the counterpart of a Rankine–Hugoniot jump condition at a shock and the similar integral relation at a fan; see also Gavrilyuk et al. (2020). For both Problems 2 and 3 we calculate the rate of increase of the oscillatory energy, and compare them with the dissipation rate at the shock in Problem 1. The results are discussed in Section 5.

2. Impact problem for a one-dimensional elastic continuum

In this section we consider the motion of a semi-infinite, one-dimensional, elastic bar. A generic particle is identified by its location $x \geq 0$ in a stress-free reference configuration. It is located at $y(x,t)$ at time t. The strain $\gamma(x,t)$, particle speed $v(x,t)$ and stress $\sigma(x,t)$ satisfy the equations

$$\gamma = y_x - 1, \quad v = y_t, \quad \sigma_x = \rho v_t, \qquad x \geq 0,\ t \geq 0, \tag{1}$$

where the subscripts x and t denote partial differentiation and ρ is the constant mass density per unit reference length. In addition, σ and γ are related by the constitutive relation

$$\sigma = W'(\gamma), \tag{2}$$

where W is the strain energy per unit reference length.[2]

Suppose that the motion involves a shock wave (whose image in the reference configuration is) at $x = s(t)$. The displacement field is continuous at the shock but the stress, strain and particle speed are permitted to be discontinuous, with their limiting values satisfying the jump conditions

$$\sigma^+ - \sigma^- + \rho\dot{s}(v^+ - v^-) = 0, \qquad v^+ - v^- + \dot{s}(\gamma^+ - \gamma^-) = 0. \tag{3}$$

Here $\dot{s} := ds/dt$ is the shock speed and h^+ and h^- denote the limiting values of a generic field $h(x,t)$ from $x = s(t)+$ and $x = s(t)-$ respectively. The limiting values must also obey the dissipation inequality[3]

$$\mathbb{D} := f\dot{s} \geq 0, \tag{4}$$

where the driving force f is

$$f := W(\gamma^+) - W(\gamma^-) - \frac{\sigma^+ + \sigma^-}{2}(\gamma^+ - \gamma^-); \tag{5}$$

e.g., see Abeyaratne and Knowles (2006) and Truskinovsky (1982). Some background on the derivation and interpretation of (4) and (5)

[2] Therefore σ has the dimension of force.

[3] Eq. (15) shows, within the context of a particular problem, why $\mathbb{D}$ is the dissipation rate.

can be found in Section S1 of the electronic supplemental material. It follows from (3) that the shock speed can be expressed as

$$\dot{s} = \pm\sqrt{\frac{1}{\rho}\,\frac{\sigma^+ - \sigma^-}{\gamma^+ - \gamma^-}}. \tag{6}$$

Dissipation in an elastic material is only possible in the presence of a changing reference configuration due, for example, to the motion of a singularity such as a shock wave, phase boundary or crack tip.

The three problems to be studied in this paper will be described in the next and subsequent sections. In order to compare the exact solution to Problem 1 with the numerical solution to Problem 2 and the approximate solution to Problem 3, we now introduce the particular elastic material characterized by

$$W(\gamma) = \frac{1}{2}\mu\gamma^2 + \frac{1}{6}\alpha^2\gamma^3, \qquad \sigma = W'(\gamma) = \mu\gamma + \frac{1}{2}\alpha^2\gamma^2, \qquad \mu > 0,\ \alpha \neq 0, \tag{7}$$

where we shall only be concerned with positive strains $\gamma > 0$. The stress–strain curve corresponding to $(7)_2$ rises monotonically and is convex. We take it to be monotonic so as to avoid phase transition fronts and convex so that the shocks are admissible according to the Oleinik criterion (Oleinik, 1959) as well as the dissipation inequality (4). For this material, the driving force (5) takes the explicit form

$$f = \frac{\alpha^2}{12}(\gamma^- - \gamma^+)^3, \tag{8}$$

and the shock speed (6) can be written as

$$\frac{\dot{s}}{c_0} = \pm\sqrt{1 + \frac{\gamma^+ + \gamma^-}{2\beta_0^2}}, \tag{9}$$

where we have set

$$\beta_0 := \sqrt{\mu/\alpha^2}, \qquad c_0 := \sqrt{\mu/\rho}\,; \tag{10}$$

c_0 is the acoustic speed in the reference configuration and β_0 measures the relative strength of the nonlinearity. The dissipation inequality (4) with (8) implies that we should take the positive square root in (9) if $\gamma^- > \gamma^+$ and the negative square root in the opposite case.

2.1. Problem 1

Problem 1 concerns the aforementioned elastic bar. The bar is unstressed and at rest at the initial instant $t = 0$ and its free-boundary $x = 0$ is subjected to a constant "pulling" speed V for all time $t > 0$. Thus we are concerned with the initial and boundary conditions

$$\gamma(x,0) = 0, \quad v(x,0) = 0, \quad x > 0 \qquad \text{and} \qquad v(0,t) = -V, \quad t > 0. \tag{11}$$

We shall refer to $V > 0$ as the "impact speed".

For a material whose stress–strain relation increases monotonically and is convex,[4] the solution to this problem has the piecewise constant form

$$\gamma(x,t), v(x,t) = \begin{cases} \gamma^-,\ -V, & 0 < x < \dot{s}t, \\ 0,\ 0, & x > \dot{s}t, \end{cases} \tag{12}$$

involving a shock wave at $x = \dot{s}t$ that moves into the undisturbed material at a constant speed $\dot{s}$. Thus the particle x remains unstrained and at rest for times $0 < t < x/\dot{s}$; its strain and speed jump instantaneously to the values γ^- and $-V$ as the shock passes through this point; and they remain at those values for $t > x/\dot{s}$. The shock speed, $\dot{s}$, and the strain behind the shock, γ^-, are to be determined.

The parameters $\dot{s}$ and γ^- can be determined from the jump conditions (3) with $\gamma^+ = 0, v^+ = 0$. For the constitutive relation (7), they tell us that the shock speed $\dot{s}(V)$ is the real positive root of the cubic equation

$$\left(\frac{\dot{s}}{c_0}\right)^3 - \frac{\dot{s}}{c_0} - \frac{1}{2}\frac{V}{c_0\beta_0^2} = 0, \tag{13}$$

and that the strain $\gamma^-(V)$ behind the shock is related to the impact speed V through either of the equivalent expressions

$$\gamma^-(V) = \frac{V}{\dot{s}(V)}, \qquad \frac{V}{c_0\beta_0^2} = \frac{\gamma^-(V)}{\beta_0^2}\sqrt{1 + \frac{1}{2}\frac{\gamma^-(V)}{\beta_0^2}}. \tag{14}$$

The relation $(14)_2$ between $\gamma^-(V)$ and V is monotonic and so there is a one-to-one relation between the impact speed and the strain behind the shock.

As pointed out to us by the reviewers, the "wave curve", the relation between V and γ^- when the states $(\gamma, v) = (0,0)$ and $(\gamma, v) = (\gamma^-, -V)$ are connected by a fan, agrees closely with the "shock curve" described by (14) over a wide range of the shock strength γ^-/β_0^2. This is generally true for weak shocks as described in Section 72 of Courant and Friedrichs (1978). More details, including a figure, can be found in Section S2 of the electronic supplemental material.

Let X be an arbitrary fixed point in the bar and limit attention to times $t < X/\dot{s}$ so that this point lies *ahead* of the shock wave. Then it can be readily shown from (1), (2), (3) and $(11)_3$ that

$$\sigma(0,t)\,V = \frac{d}{dt}\int_0^X E(x,t)\,dx \ + \ \mathbb{D}, \qquad E(x,t) := \frac{1}{2}\rho v^2(x,t) + W(\gamma(x,t)), \tag{15}$$

where $\mathbb{D}$ is given by (4), (5). The left-hand side of $(15)_1$ represents the rate of external working on the segment $[0, X]$ of the bar and the first term on its right-hand side is the rate of increase of the kinetic plus potential energy of this segment. Therefore $\mathbb{D}$ represents the rate of dissipation. The fact that $\mathbb{D} \neq 0$ is due to the presence of the shock wave within the interval $[0, X]$. From (4), (8), (9) with $\gamma^+ = 0$, the dissipation rate $\mathbb{D} = f\dot{s}$ in Problem 1 can be written as

$$\frac{\mathbb{D}}{\mu c_0 \beta_0^4} = \frac{1}{12}\left(\frac{\gamma^-}{\beta_0^2}\right)^3\sqrt{1 + \frac{1}{2}\frac{\gamma^-}{\beta_0^2}}. \tag{16}$$

3. Impact problem for a discrete system of particles

We now consider a semi-infinite chain of identical particles numbered $j = 0, 1, 2, \ldots$, each of mass m. The jth particle is located at $x_j = hj$ in a reference configuration and at $y_j(t)$ at time t. Each particle interacts with its nearest neighbors (only) through identical nonlinear elastic springs. We shall refer to the spring connecting the jth and j+1th particles as the jth spring. The particle speed, v_j, and the elongation of the jth spring, δ_j, are

$$v_j = \dot{y}_j, \qquad \delta_j = y_{j+1} - y_j - h. \tag{17}$$

If $U(\delta_j)$ denotes the potential energy of the jth spring, the force in that spring is

$$\sigma_j = U'(\delta_j), \tag{18}$$

and a motion of the particle chain is described by the system of equations

$$m\dot{v}_j = U'(\delta_j) - U'(\delta_{j-1}), \qquad \dot{\delta}_j = v_{j+1} - v_j. \tag{19}$$

In order to compare the solutions of the discrete and continuous systems, we let

$$\gamma_j(t) := \delta_j(t)/h, \tag{20}$$

be the strain in the jth spring and introduce the energy per unit reference length, W, expressed as a function of strain:

$$W(\gamma_j) := U(h\gamma_j)/h. \tag{21}$$

[4] If the stress–strain relation is monotonic and concave, the strain and particle speed vary continuously and the solution involves a fan, $\gamma = \gamma(x/t), v = v(x/t)$, connecting two constant states.

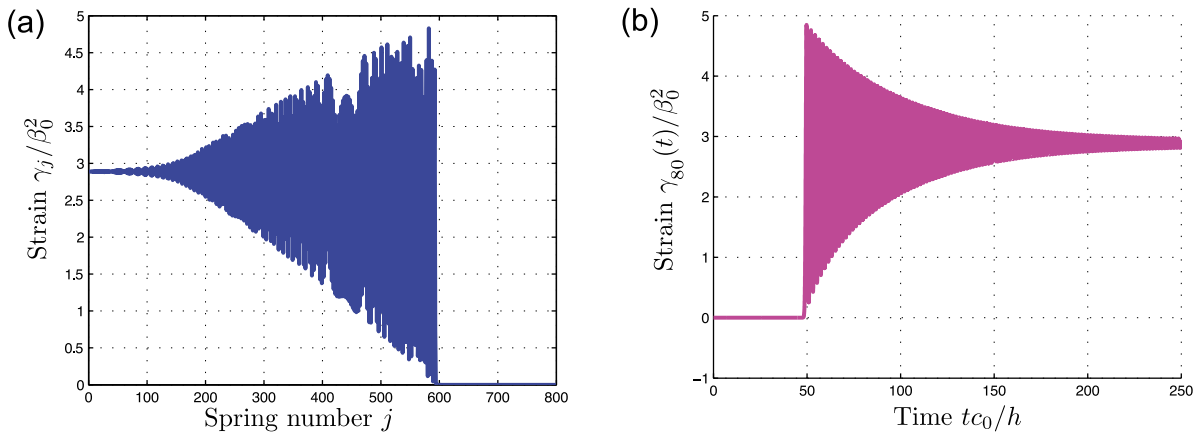

Fig. 1. (*a*) Strain $\gamma_j(t)/\beta_0^2$ versus spring number j at time $tc_0/h = 360$. (*b*) Strain $\gamma_{80}(t)/\beta_0^2$ versus time tc_0/h at spring $j = 80$. The value of the strain in a spring remains at zero for a certain initial period of time, undergoes a rapid increase when the disturbance wave reaches it, and then undergoes rapid oscillations with slowly decaying amplitude. The amplitude of oscillation decreases linearly in (*a*) and "curvilinearly" in (*b*). For these plots $V/(c_0\beta_0^2) = 4.48$, $N = 800$. The associated x,t-plane is shown schematically in Fig. 2.

It follows that the force in the jth spring is $\sigma_j = U'(\delta_j) = W'(\gamma_j)$ where the prime denotes differentiation with respect to the argument. We also let

$$\rho = m/h. \tag{22}$$

Let E_j denote the total energy of the jth spring–particle pair, i.e. the kinetic energy of the jth particle plus the potential energy of the jth spring:

$$E_j := \frac{1}{2}\, m v_j^2 + U(\delta_j). \tag{23}$$

The following balance equation can be *derived* from (19):

$$U'(\delta_j)v_{j+1} - U'(\delta_{j-1})v_j = \frac{dE_j}{dt}, \qquad j = 1, 2, \dots\ . \tag{24}$$

Considering the jth spring–particle pair as a system, Eq. (24) states that the rate-of-working of the external forces on this system equals the rate of increase of its energy.

3.1. Problem 2

Problem 2 is the discrete counterpart of Problem 1 and concerns the aforementioned chain of particles. At the initial instant the particles are at rest and the springs are unstretched. For all time $t > 0$ the zeroth particle is subjected to a constant "pulling" speed $V > 0$ (and we again refer to it as the "impact speed"). Thus we are concerned with the initial and boundary conditions

$$v_j(0) = 0,\ j = 1, 2, \dots; \qquad \delta_j(0) = 0,\ j = 0, 1, 2, \dots; \qquad v_0(t) = -V,\ t > 0. \tag{25}$$

The initial boundary-value problem (19), (25) was solved numerically for a chain with N particles for the material characterized by

$$U(\delta) = h\left[\frac{1}{2}\mu\left(\frac{\delta}{h}\right)^2 + \frac{1}{6}\alpha^2\left(\frac{\delta}{h}\right)^3\right], \qquad \mu > 0, \alpha \neq 0; \tag{26}$$

cf. (26) with $(7)_1$, (21); the associated acoustic speed is

$$c_0 := \sqrt{\mu h/m} \overset{(22)}{=} \sqrt{\mu/\rho}. \tag{27}$$

We used the ode45 integrator in MATLAB, which is based on the Runge–Kutta method (Dormand and Prince, 1980; Shampine and Reichelt, 1997), to compute the solution, and stopped calculations before any waves reached the remote end of the chain. To confirm the results, we repeated these calculations using a leap frog integrator, Frenkel and Smit (2002). The relative difference in the results, e.g. for the energy, was less than 0.35%.

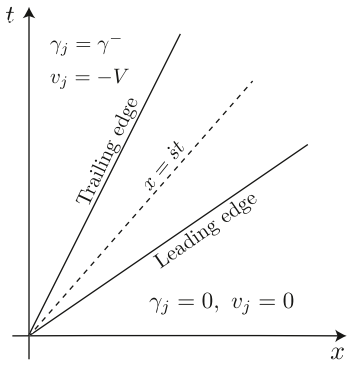

Fig. 2. The schematic x,t-plane for Problem 2. The dispersive wave packet is contained between the leading and trailing edges. The dashed ray $x = \dot{s}t$ corresponds the shock wave in Problem 1.

Fig. 1 shows how the strain of the jth spring varies with the spring number j (at a fixed time t) and with time t (at a fixed spring j) in one (arbitrarily chosen) calculation. The strain in a spring remains at the value zero for a certain initial period of time, undergoes a rapid increase when the disturbance wave reaches it, and then undergoes rapid oscillations with slowly decaying amplitude. The x,t-plane associated with this dispersive shock wave is shown schematically in Fig. 2. The dispersive wave packet is contained between the two rays corresponding to its leading and trailing edges. The dashed ray $x = \dot{s}t$ corresponds to the shock wave in Problem 1.

Note from Fig. 1(b) that there are two time-scales involved: the slow time on which the amplitude decreases and the fast time on which the oscillations occur. Observe also that the amplitude of oscillation as a function of j decreases linearly (Fig. 1(*a*)), whereas as a function of t it decreases "curvilinearly" (Fig. 1(*b*)). We shall revisit this observation in Section S9.

Fig. 3 shows the results of a few such calculations. Observe that the solution involves a dispersive wave packet propagating into the quiescent material. The amplitude of oscillation at the leading edge remains constant as the wave packet propagates, but its width increases with time since the leading edge travels faster than the trailing edge.

Several such calculations were carried out, and from them, we observed that for each spring j,

$$\langle \gamma_j(t) \rangle \ \to\ \overline{\gamma} \qquad \text{as} \quad t \to \infty; \tag{28}$$

i.e. the strain $\gamma_j(t)$ in every spring j approaches a value $\overline{\gamma}$ (independent of j) in the sense of a weak limit, meaning that the strain approaches

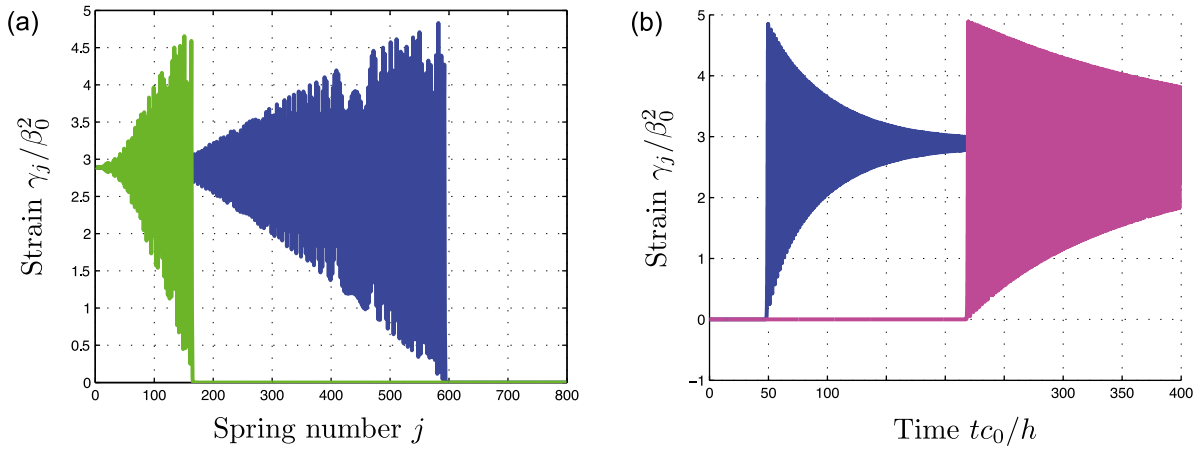

Fig. 3. Strain profiles: (*a*) strain $\gamma_j(t)/\beta_0^2$ versus spring number j at two times $tc_0/h = 100$ (left), $tc_0/h = 360$ (right). (*b*) Strain $\gamma_j(t)/\beta_0^2$ versus time tc_0/h for two springs, $j = 80$ (left) and $j = 360$ (right). For these plots, $V/(c_0\beta_0^2) = 4.48$, $N = 800$. The associated x,t-plane is shown schematically in Fig. 2.

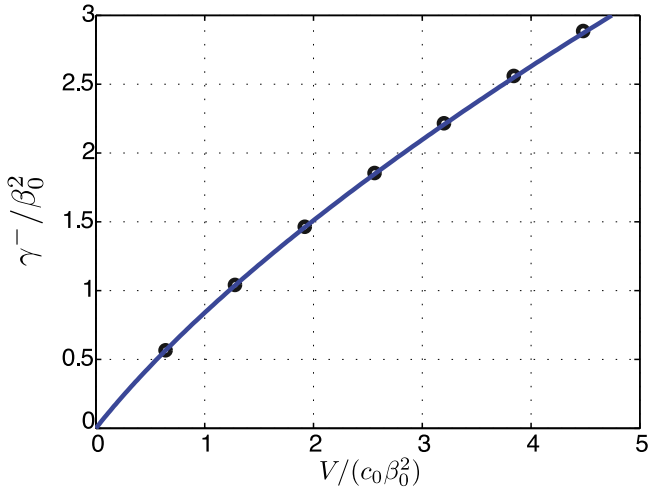

Fig. 4. The circles correspond to the limiting strain $\overline{\gamma}/\beta_0^2$ in Problem 2 as determined numerically while the solid curve corresponds to the strain γ^-/β_0^2 behind the shock in Problem 1 according to $(14)_2$.

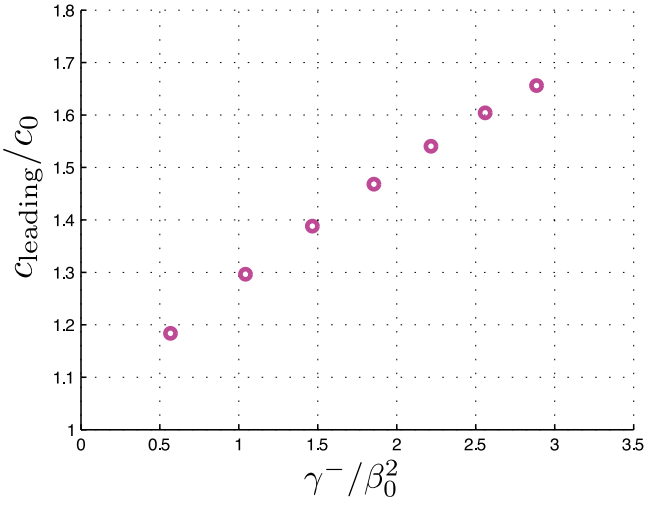

Fig. 5. The speed c_{leading} of the leading edge of the wave packet in Problem 2 determined numerically.

an average value $\overline{\gamma}$ upon which are superposed periodic oscillations. In this paper, whenever we say that some quantity approaches a certain value, it will always be in this sense of a weak limit unless explicitly stated otherwise. The particle speed $v_j(t)$ similarly approaches the value $v_0 = -V$ at each j where V is the impact speed.

The limiting strain value $\overline{\gamma}$ is independent of spring number and time but depends on the impact speed. Since $\overline{\gamma}$ is found by solving a different set of equations to those in Problem 1, it is not a priori necessary that it equal the strain γ^- behind the shock wave in Problem 1. The circles in Fig. 4 show how $\overline{\gamma}$ varies with V according to our numerical solution of Problem 2. The variation of the strain γ^- in Problem 1 according to $(14)_2$ corresponds to the solid curve. It is difficult to distinguish between the two from the figure, the relative difference between the values of strain being less than 0.5%. This is consistent with the former problem being the discrete counterpart of the latter. From hereon we shall write γ^- for $\overline{\gamma}$.

We next determine the speed of the leading edge of the propagating wave packet, c_{leading}, or equivalently the spring number, $n(t)$, of the spring at the leading edge. This will be needed in the next section. We identify the spring at the leading edge using the criterion that it is the first spring in the chain whose strain has risen from 0 and exceeded the (ad hoc) threshold value 1.0×10^{-8}. The speed of the leading edge is then given by $c_{\text{leading}} = \dot{n}h$. We estimated c_{leading} for various values of the impact speed V (or equivalently the strain γ^-). The results are displayed in Fig. 5.

The chain of particles connected by nonlinear elastic springs is a conservative system. In fact, upon summing (24), one is led to

$$\sigma_0 V = \frac{dE}{dt}, \qquad E(t) := \sum_{j=0}^{\infty} E_j(t), \tag{29}$$

where $\sigma_0(t) = U'(\delta_0(t))$ is the externally applied force on the zeroth particle[5]; $v_0(t) = -V$ is its speed; $\dot{E}_0 = U'(\delta_0)\dot{\delta}_0$ which follows from (23) with $\dot{v}_0 = 0$; and E is the total energy in the system.[6] Eq. (29) is simply a statement of the usual elastic power identity ("conservation of energy") and should be compared with the corresponding Eq. (15) for the elastic bar which involves an additional dissipative term.

[5] Since the zeroth particle travels at constant speed, the resultant force on it vanishes and therefore the externally applied force on it equals the force in the zeroth spring.

[6] We assume that the infinite sum in $(29)_2$ converges for the particular motions involved in Problem 2.

While the theory implies that (29) must necessarily hold, not all numerical schemes conserve energy. In fact, the decaying strain amplitudes in Figs. 1 and 3 are reminiscent of the oscillations of a *damped* system. For our purposes, where the calculation of energy underlies the central question being investigated, it is important that the discreteness of the particle chain not introduce any numerical dissipation. As described in Section S3 of the electronic supplemental material, we confirmed that the numerical scheme used conserved energy and obeyed (29). The relative difference between the rate of change of energy and the rate of working shown in Figure S2 was less than 0.3%.

3.2. Oscillatory energy. Apparent dissipation

Energy is not conserved in Problem 1 because of the propagating shock wave, while energy is conserved in its discrete counterpart Problem 2. One way to heuristically understand the dissipation in Problem 1 in terms of the energy in Problem 2 is as follows: the strain and speed of all particles in the chain eventually settle at the values γ^- and $v^- = -V$. This motivates us to introduce

$$v_j^{\rm osc}(t) := v_j(t) - v^-, \qquad \gamma_j^{\rm osc}(t) := \gamma_j(t) - \gamma^- \qquad \text{for} \quad 0 \le j \le n(t), \tag{30}$$

where $n(t)$ is the particle at the leading edge of the propagating wave packet at time t. We define the energy associated with the oscillatory part of the motion by

$$E_{\rm osc}(t) := \sum_{j=0}^{n(t)} \left(\frac{1}{2}\, m\big(v_j^{\rm osc}(t)\big)^2 + hW(\gamma_j^{\rm osc}(t)) \right), \tag{31}$$

and refer to it as the oscillatory energy in the system. Then the rate of increase of the oscillatory energy is

$$D(t) = \frac{d}{dt} E_{\rm osc}(t). \tag{32}$$

We calculated D using (32) as follows: for each impact speed V, we calculated the oscillatory energy $E_{\rm osc}(t)$ using the numerical solution to the problem together with (30) and (31); the particle $n(t)$ at the leading edge was determined by finding the first spring whose strain has risen above the threshold value of 1×10^{-8} as described in Section 3.1. We then plotted $E_{\rm osc}(t)$ versus t and observed that the relationship was linear (with small superposed jagged oscillations). We identified D with the slope of this line which is effectively an averaging over the rapid oscillations.[7] Several such calculations were carried out for different values of the impact speed V.

The circles in Fig. 6 show the variation of D with the impact speed V in Problem 2. The solid curve corresponds to the dissipation-rate $\mathbb{D}$ in Problem 1 as given by (16). These results will be discussed in Section 5.

4. Impact problem for a dissipationless dispersive continuum

Since the solution to the impact problem for the discrete chain (Problem 2) displays dispersion but no dissipation, we now turn to a continuum model that has these same two characteristics. Specifically, we add a strain-gradient term to the stress–strain relation $(7)_2$ of Problem 1, and thus take the constitutive relation of the one-dimensional semi-infinite continuum to be

$$\sigma = W'(\gamma) + \eta h^2 \gamma_{xx}, \qquad W(\gamma) = \frac{1}{2}\mu\gamma^2 + \frac{1}{6}\alpha^2\gamma^3; \tag{33}$$

here $\eta > 0$ and $h > 0$ are constant parameters.

Taking $\eta > 0$ in (33) is motivated by Taylor expanding the discrete equations of Problem 2 for small h; e.g. $\eta/\mu = 1/12$ according to Rosenau (1986). However, $\eta > 0$ leads to instability at perturbations whose wave lengths are smaller than some critical value. As noted by Sharma (2005), despite this deficiency, interesting results can be derived in this case, Kresse and Truskinovsky (2003), Abeyaratne and Vedantam (1999, 2003). In the context of the present problem, we show in the appendix that if we limit attention to perturbations whose wave lengths remains close to the wave lengths of the solutions encountered here, then stability is maintained.

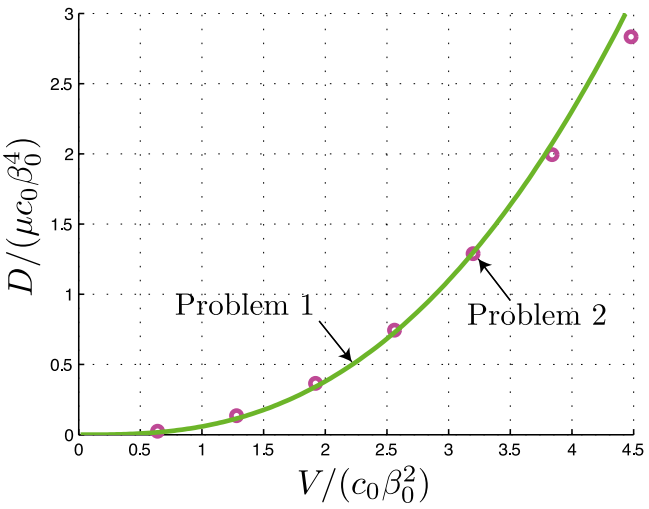

Fig. 6. The circles correspond to the oscillatory energy $D/(\mu c_0\beta_0^4)$ in Problem 2 while the solid curve corresponds to the dissipation-rate $\mathbb{D}/(\mu c_0\beta_0^4)$ in Problem 1 according to (16), $(14)_2$.

Consider a motion $y(x,t) = x + u(x,t)$ where $u(x,t)$ is the displacement of particle x at time t. We do *not* assume u or its derivatives to be small. The strain and particle speed associated with this motion are $\gamma = y_x - 1 = u_x, v = y_t = u_t$. Substituting $(33)_1$ into the equation of motion $\sigma_x = \rho v_t$, and from the definitions of strain and particle speed, one obtains the following pair of partial differential equations for $\gamma(x.t), v(x,t)$:

$$\eta_0 h^2 \gamma_{xxx} + \gamma_x + \beta_0^{-2}\gamma\gamma_x = c_0^{-2} v_t, \qquad v_x = \gamma_t. \tag{34}$$

Here we have set

$$\eta_0 = \eta/\mu,$$

and $c_0 = \sqrt{\mu/\rho}$ and $\beta_0 = \sqrt{\mu/\alpha^2}$ as before.

The system of Eqs. (34) is closely related to the Boussinesq equation studied, for example, by Ratliff and Bridges (2016) and Nguyen and Smyth (2021); see also Section 13.11 of Whitham (1974). Based on the analyses of those equations, as well as the numerical solution to Problem 2, we expect the impact problem for the dissipationless, dispersive system (34) to involve a modulated traveling wave packet in which the amplitude of oscillation decays slowly, much more slowly than the time-scale associated with the frequency of oscillation.

The mathematical theory for constructing such solutions was put forward by Whitham (1965b, 1970) and has since been further developed and used by many authors, e.g. see the review article by El and Hoefer (2016), the dissertation by Nguyen (1987), the book by Kamchatnov (2000) and the references therein. The first step in this procedure is to construct an exact *periodic* traveling wave solution, and in the second step, to allow the parameters in that solution to vary slowly in an appropriate manner according to the so-called modulation equations. For example, the periodic traveling wave may have the form $\hat{\gamma}((kx - \omega t)/\epsilon, p)$ where k, ω and p are constant parameters, with the modulated wave having the form $\hat{\gamma}(\theta(x,t)/\epsilon, p(x,t))$ where $\theta(x,t)$ and $p(x,t)$ are slowly varying functions and $\epsilon \ll 1$. Such waves involve two slow scales x and t and two fast scales x/ϵ and t/ϵ. When $\epsilon = 0$, the underlying system of partial differential equations is hyperbolic and its solution can involve a shock wave (as in Problem 1). The term $\epsilon > 0$

[7] Figure S3 in Section S4 of the electronic supplemental material shows a graph of $E_{\rm osc}(t)$ versus t.

introduces dispersion into the problem (but not dissipation) and the solution corresponding to a shock wave is a dispersive shock wave.

4.1. Steady periodic traveling wave

Motivated by this, we first seek a steady periodic traveling wave solution of (34) of the form

$$\gamma(x,t) = g(\Phi), \quad v(x,t) = w(\Phi), \qquad \Phi = \frac{kx-\omega t}{h}, \qquad c = \omega/k, \tag{35}$$

where the wave number k, frequency ω and phase speed c are constants (for the moment). From (34) and (35) we obtain

$$\eta_0 k^2 g''' + g' + \beta_0^{-2} g g' = -(c/c_0^2) w', \qquad w' = -c g'. \tag{36}$$

Integrating $(36)_2$ gives $w(\Phi) = -c g(\Phi) + v_*$, where v_* is a constant (for the moment). Thus, and by substituting $(36)_2$ into $(36)_1$, we can rewrite (36) as the following pair of equations for $g(\Phi)$ and $w(\Phi)$:

$$\eta_0 k^2 g''' - (c^2/c_0^2 - 1) g' + \beta_0^{-2} g g' = 0, \qquad w(\Phi) = v_* - c\, g(\Phi). \tag{37}$$

The strain and particle speed in the traveling wave can now be expressed as

$$\gamma(x,t) = g(\Phi), \qquad v(x,t) = v_* - c\, g(\Phi), \qquad \Phi = \frac{kx-\omega t}{h}. \tag{38}$$

Once a traveling wave solution for the strain is determined from $(37)_1$, the associated traveling wave for the particle speed is given immediately by $(37)_2$ to within the arbitrary constant v_*.

Integrating $(37)_1$ twice leads to

$$\left(g'\right)^2 = \frac{1}{3\kappa^2}\left[d_1 + d_2\, g + 3\beta_0^2 (c^2/c_0^2 - 1) g^2 - g^3\right], \tag{39}$$

where d_1 and d_2 are constants of integration and

$$\kappa := k\beta_0\sqrt{\eta_0}. \tag{40}$$

With the exception of the coefficient in front of the term g^2, Eq. (39) is the same equation that is arrived at when studying periodic traveling waves in the Korteweg–de Vries (KdV) equation. We shall therefore simply write down the relevant solution of (39) and list its key features without derivation and refer the reader to the literature on DSWs in the KdV equation for details, e.g. Section IV-B of Hoefer et al. (2006).

A three-parameter family of 2π-periodic solutions of (39) is

$$g(\Phi) = g^- - m^2(g^- - g^+) + 2m^2(g^- - g^+)\mathrm{cn}^2\left(\frac{K(m)}{\pi}\Phi; m\right), \tag{41}$$

where $\mathrm{cn}(z,m)$ is a Jacobi elliptic function,[8] $K(m)$ is the complete elliptic integral of the first kind, and the three constant parameters g^-, g^+ and m are arbitrary except for the requirements

$$g^- > g^+, \qquad 0 \le m \le 1.$$

The associated phase speed c, wave number k and group speed V_g are

$$\frac{c}{c_0} = \sqrt{1 + \left[\frac{2g^+ + g^- + m^2(g^- - g^+)}{3\beta_0^2}\right]}, \tag{42}$$

$$k = \frac{\pi}{K(m)}\sqrt{\frac{g^- - g^+}{6\eta_0\beta_0^2}}, \tag{43}$$

$$\frac{V_g}{c_0} = \frac{c_0}{c}\left[\frac{c^2}{c_0^2} - \frac{mK(m)}{K'(m)}\frac{g^- - g^+}{3\beta_0^2}\right], \tag{44}$$

where $K'(m)$ is the derivative of $K(m)$ with respect to m. The function $\mathrm{cn}^2[\cdot, m]$ oscillates between the values 0 and 1 and so the (peak to valley) amplitude of oscillation in (41) is

$$a = 2m^2(g^- - g^+). \tag{45}$$

[8] Definitions and properties of this and the other elliptic functions encountered in this paper can be found, for example, in Byrd and Friedman (1972), Olver et al. (2021). It should be noted that the parameter we call m^2 is taken by some authors, including MATHEMATICA, to be m.

The three parameters g^+, g^- and m can of course be replaced by the three "physical parameters", phase speed c, wave number k and amplitude a. Note that the amplitude, phase speed and group speed do not depend on the strain-gradient parameter η but the wave number does.

It will be useful for future purposes to note that the average of $g(\Phi)$ over the oscillations, defined by

$$\langle g \rangle := \frac{1}{2\pi}\int_0^{2\pi} g(\Phi)\, d\Phi, \tag{46}$$

is

$$\langle g \rangle = 2g^+ - g^- + m^2(g^- - g^+) + 2(g^- - g^+)\frac{E(m)}{K(m)}, \tag{47}$$

where $E(m)$ is the complete elliptic integral of the second kind.

Turning next to the particle speed, the periodic traveling wave solution is obtained immediately by substituting (41) into $(37)_2$ which gives

$$w = w^- - m^2(w^- - w^+) + 2m^2(w^- - w^+)\mathrm{cn}^2\left(\frac{K(m)}{\pi}\Phi; m\right), \tag{48}$$

where

$$w^- = v_* - c g^-, \qquad w^+ = v_* - c g^+. \tag{49}$$

This involves four constant parameters, three of which (g^-, g^+ and m) are the same as in the solution for the strain. The fourth parameter v_* is an additional arbitrary constant. The phase speed c appearing in (49) is known in terms of g^-, g^+ and m; see (42). The average value of $w(\Phi)$ is

$$\langle w \rangle = v_* - c\langle g \rangle = 2w^+ - w^- + m^2(w^- - w^+) + 2(w^- - w^+)\frac{E(m)}{K(m)}. \tag{50}$$

4.2. Slow modulation of the periodic traveling wave solution. Dispersive shock wave (DSW)

4.2.1. Strain field $\gamma(x,t)$

The next step according to modulation theory, would be to construct a slow modulation of the preceding periodic traveling wave solution for the strain field, by allowing the three parameters g^-, g^+ and m in (41) to be slowly varying functions of x and t, and to determine them from the modulation equations. These equations are to be obtained by either the singular perturbation method of two-timing, variational methods, or averaging three supplementary conservation laws, (Whitham, 1965b,a, 1967, 1970).

We, however, we will not implement this second step exactly. Rather than allowing all three of $g^\pm$ and m to be slowly varying fields, we shall only permit m to be slowly varying and assume $g^\pm$ to be constant. Consider the parameter m that is required to be in the range $0 \le m \le 1$. If $m(x,t)$ varies from 0 to 1 as one moves from the trailing edge to the leading edge of the wave packet, according to (45) the amplitude of oscillation would increase from 0 to $2(g^- - g^+) > 0$ (qualitatively as in Fig. 3). Next, from (47) and the properties of the complete elliptic integrals $E(m)$ and $K(m)$,

$$\langle g \rangle \to g^- \quad \text{as} \quad m \to 0, \qquad \langle g \rangle \to g^+ \quad \text{as} \quad m \to 1, \tag{51}$$

and so the average value of g varies from g^- to g^+ when m varies from 0 to 1. In view of these observations, and since we will eventually be interested in a solution that connects two *constant states, we make the ad hoc assumption that the two parameters* g^- *and* g^+ *remain constant and only* $m = m(x,t)$ *is slowly varying.* This assumption is not based on modulation theory. Observe from the relevant formulae in the preceding sub-section that the amplitude, wave number, group speed etc. are all functions of m (but not Φ) and so they will vary slowly.

We make one more set of observations before turning to finding $m(x,t)$. Since m ranges over the interval $[0,1]$, it is useful to look at the solution (41) in the two limiting cases $m \to 0$ and $m \to 1$. When $m \to 1$

one can show from (43) that $k \to 0$ (so that the wave length $\to \infty$) and that $g(\Phi)$ is described by the soliton

$$g(\Phi) = g^+ + 2(g^- - g^+)\mathrm{sech}^2\left(\frac{K(m)}{\pi}\Phi\right).$$

According to (42) with $m = 1$, the soliton propagates at the particular phase speed

$$\frac{c_{\text{soliton}}}{c_0} := \sqrt{1 + \frac{g^+ + 2g^-}{3\beta_0^2}}. \tag{52}$$

In the limit $m \to 0$ one sees that $g(\Phi)$ is described by the constant solution

$$g(\Phi) = g^-. \tag{53}$$

For small m one has

$$g(\Phi) \sim g^- + \frac{a}{2}\cos\Phi, \qquad a = 2m^2(g^- - g^+),$$

which is a harmonic wave propagating, according to (42), at the phase speed

$$\frac{c_{\text{harmonic}}}{c_0} := \sqrt{1 + \frac{2g^+ + g^-}{3\beta_0^2}}. \tag{54}$$

It is worth noting from (43) and $(51)_1$ that near the trailing edge of the DSW where m is small, one has

$$\eta_0 k^2 \sim \frac{2}{3}\frac{g^- - g^+}{\beta_0^2}, \qquad \langle g\rangle \sim g^-.$$

Consequently

$$\frac{c_{\text{harmonic}}^2}{c_0^2} \sim 1 + \frac{\langle g\rangle}{\beta_0^2} - \eta_0 k^2,$$

which is precisely the dispersion relation of the system (34) linearized about the uniform state $\gamma = \langle g\rangle$, $v = \langle v\rangle$.

A curious factoid is that if one sets $g^+ = \gamma^+$ and $g^- = \gamma^-$ in (52) and (54), one finds that the speed $\dot{s}$ of the shock wave in the elastic continuum (as given in (9)) is related to the phase speeds c_{soliton} and c_{harmonic} by

$$\dot{s}^2 = \frac{1}{2}(c_{\text{soliton}}^2 + c_{\text{harmonic}}^2).$$

We now turn to determining the function $m(x,t)$, and for this we need another equation. This equation is obtained by one of the methods mentioned in the first paragraph of this sub-section. One of the equations that typically arises from all such derivations is the so called *conservation of waves* equation,

$$\frac{\partial\omega}{\partial x} + \frac{\partial k}{\partial t} = 0, \tag{55}$$

relating the frequency and wave number, $\omega(x,t)$ and $k(x,t)$, of the modulated wave. We take for granted that (55) is the requisite additional equation. Since $V_g = d\omega/dk$, this can alternatively be written as $\partial k/\partial t + V_g\,\partial k/\partial x = 0$ which is the usual statement that wave numbers propagate at the group speed. Since $k(x,t)$ varies only due to the variation of $m(x,t)$, i.e. k is a function of m, this in turn leads to

$$\frac{\partial m}{\partial t} + V_g(m)\frac{\partial m}{\partial x} = 0, \tag{56}$$

where $V_g(m)$ is the group speed given by (44); terms involving $\partial g^+/\partial x$ and $\partial g^-/\partial x$ will appear in (56) had we not made the assumption that g^+ and g^- are constants. Once (56) (with initial/boundary conditions as needed) has been solved for $m(x,t)$, the solution $g(x,t)$ is given by (41).

Finally, in light of the particular problem we want to study, we restrict attention to the case where m is scale-invariant so that $m(x,t) = m(x/t)$. Then (56) reduces to the algebraic equation

$$\frac{x}{t} = V_g(m). \tag{57}$$

Upon using (44) this can be written explicitly as

$$\frac{x}{t} = \frac{c_0^2}{c(m)}\left[\frac{c^2(m)}{c_0^2} - \frac{1}{\beta_0^2}\frac{mK(m)}{K'(m)}\frac{g^- - g^+}{3}\right], \tag{58}$$

where the phase speed $c(m)$ is given by (42). Eq. (58) gives x/t as a function of m, whose inverse yields $m = m(x/t)$.

Thus in summary, the strain field $\gamma(x,t)$ in the DSW is given by

$$\gamma(x,t) = g^- - m^2(g^- - g^+) + 2m^2(g^- - g^+)\mathrm{cn}^2\left(\frac{K(m)}{\pi}\Phi; m\right), \tag{59}$$

where $m = m(x/t)$ is determined by inverting (58). The parameters g^+ and g^- are constants and $\Phi = k(m)(x - c(m)t)/h$ with $c(m)$ and $k(m)$ given by (42) and (43).

4.2.2. Particle speed $v(x,t)$

In order to construct the slowly modulated wave for the particle speed we turn to (48) with $w^\pm(x,t) = v_*(x,t) - c(m(x,t))g^\pm$. Since the modification to $m(x,t)$ has already been dealt with in the preceding subsection, it remains to determine the slowly varying function $v_*(x,t)$. We again restrict attention to the special case where $v_*(x,t)$ is scale invariant: $v_* = v_*(x/t)$. However, since $x/t = V_g(m)$, we may equivalently say that $v_* = v_*(m)$ whence we can write the particle speed field as

$$v(x,t) = w^-(m) - m^2(w^-(m) - w^+(m)) + 2m^2(w^-(m) - w^+(m))\mathrm{cn}^2\left(\frac{K(m)}{\pi}\Phi; m\right), \tag{60}$$

where

$$w^\pm(m) = v_*(m) - c(m)g^\pm, \tag{61}$$

with $m(x/t)$ given by (58) and $v_*(m)$ to be determined. Observe that in the particular solution we have constructed, in contrast to $g^\pm$, the quantities $w^\pm(m)$ are not constants.

In order to find $v_*(x,t) = v_*(m)$ we average the conservation law[9] $v_x = \gamma_t$ over the fast oscillations (i.e. with respect to Φ) to get

$$\frac{\partial}{\partial x}\langle w\rangle = \frac{\partial}{\partial t}\langle g\rangle;$$

see (46) for the definition of the average and note that, since the period, 2π, of oscillation is constant, the averaging integral can be moved inside the derivatives. Since $\langle w\rangle$ and $\langle g\rangle$ depend on x,t only through $m(x/t)$, this yields $\langle\, w\,\rangle' = -V_g\,\langle\, g\,\rangle'$ where a prime denotes differentiation with respect to m and we have used (56). On using $\langle w\rangle = v_* - c\langle g\rangle$, (42) and (44) this leads to

$$v_*'(m) = \frac{g^- - g^+}{3\beta_0^2}\frac{c_0^2}{c(m)}\frac{m}{K'(m)}\frac{d}{dm}\Big(\langle g\rangle K(m)\Big),$$

which can be further simplified using (47) to

$$v_*'(m) = \frac{g^- - g^+}{3\beta_0^2}\frac{c_0^2}{c(m)}m\big[g^- - (g^- - g^+)m^2\big].$$

Finally, this can be integrated (by changing the variable of integration from m to c) to obtain

$$v_*(m) = v_*(1) + (2g^- + 2g^+ + 3\beta_0^2)(c - c_{\text{soliton}}) + (\beta_0^2/c_0^2)(c_{\text{soliton}}^3 - c^3), \tag{62}$$

having used the fact that $c = c_{\text{soliton}}$ when $m = 1$.

Thus in summary, the particle speed field $v(x,t)$ in the DSW is given by (60), (61), (62) where g^+, g^- and $v_*(1)$ are constants; $\Phi = k(m)(x - c(m)t)/h$ with $c(m)$ and $k(m)$ given by (42) and (43); and $m = m(x/t)$ is determined by inverting (58).

[9] Section S7 of the electronic supplemental material gives a set of four Lagrangian conservation laws we could use had we allowed all four parameters g^+, g^-, m and v_* to be slowly varying.

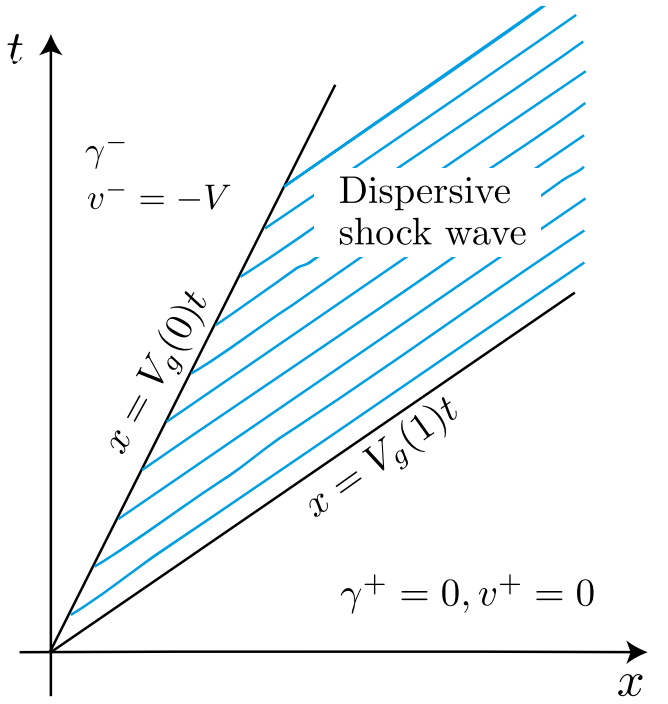

Fig. 7. The schematic x,t-plane associated with the approximate solution (Problem 3).

4.3. Problem 3

We now use the preceding modulated traveling wave to construct an approximate solution to the impact problem for the dispersive continuum under consideration. We refer to this problem as Problem 3.

Recall that the strain and particle speed can be identified with

$$\gamma(x,t) = g(x,t), \qquad v(x,t) = w(x,t) = v_*(m) - c(m)g(x,t), \qquad m = m(x/t). \tag{63}$$

We take for granted that the x,t-plane is as shown schematically in Fig. 7 where the strain and particle speeds ahead of and behind the DSW are constant and have the values, say, γ^+, v^+ and γ^-, v^- respectively. (It is instructive not to take $\gamma^+ = 0, v^+ = 0$ initially though we shall do so later.)

First consider the leading edge of the DSW. Since $m = 1$ here, it follows from (57) that the leading edge is described by $x = V_g(1)t$, and from (51) and (52) that $\langle\gamma\rangle = g^+$ and $c = c_{\text{soliton}}$ there. Thus by this and (63), the average strain and particle speed just behind the leading edge are g^+ and $\langle v\rangle = w^+(1) = v_*(1) - c_{\text{soliton}}g^+$. Matching them to the strain and particle speed ahead of the leading edge thus gives

$$g^+ = \gamma^+, \qquad w^+(1) = v_*(1) - c_{\text{soliton}}\gamma^+ = v^+. \tag{64}$$

Similarly, since $m = 0$ at the trailing edge, one has $x = V_g(0)t$, $\langle\gamma\rangle = g^-$ and $c = c_{\text{harmonic}}$ there. It therefore follows that the average strain and particle speed just inside of the trailing edge are g^- and $\langle v\rangle = w^-(0) = v_*(0) - c_{\text{harmonic}}g^-$, and so, matching across the trailing edge leads to

$$g^- = \gamma^-, \qquad w^-(0) = v_*(0) - c_{\text{harmonic}}\gamma^- = v^-. \tag{65}$$

From (64), (65), (62), (52) and (54) one obtains the following relation between $\gamma^\pm$ and $v^\pm$:

$$v^+ - v^- = 2(\beta_0^2/c_0^2)\left[c_{\text{soliton}}^3 - c_{\text{harmonic}}^3\right]; \tag{66}$$

here c_{soliton} and c_{harmonic} are given by (52) and (54) respectively. Eq. (66) is an explicit relation between the states γ^-, v^- behind the DSW and the state γ^+, v^+ ahead of it. It is the counterpart of a Rankine–Hugoniot jump condition at a shock and the corresponding integral relation at a fan.

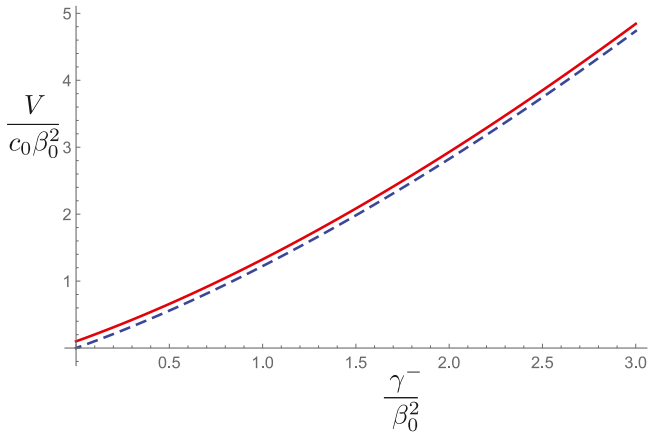

Fig. 8. The impact speed $V/(c_0\beta_0^2)$ versus the strain γ^-/β_0^2 for Problem 3 (dashed, Eq. (67)) and for Problem 1 (solid, Eq. $(14)_2$). The two curves fall on top of each other and for clarity we have shifted the curve corresponding to the shock (solid) by 0.1 units vertically. The relative difference between the predicted impact speeds, in the range considered, is less than 0.15%. The figure has been drawn for impact speeds conforming to (72) below.

In the specific problem at hand, the system is quiescent initially and so $\gamma^+ = v^+ = 0$. Behind the wave packet we have $v^- = -V$ where V is the impact speed. On using this, (66) simplifies to

$$\frac{V}{c_0} = 2\beta_0^2\left[\left(\frac{c_{\text{soliton}}}{c_0}\right)^3 - \left(\frac{c_{\text{harmonic}}}{c_0}\right)^3\right], \tag{67}$$

where c_{soliton} and c_{harmonic} specialize to

$$\frac{c_{\text{soliton}}}{c_0} := \sqrt{1 + \frac{2\gamma^-}{3\beta_0^2}}, \qquad \frac{c_{\text{harmonic}}}{c_0} := \sqrt{1 + \frac{\gamma^-}{3\beta_0^2}}. \tag{68}$$

This is an implicit algebraic equation for determining the strain γ^- behind the DSW corresponding to the given impact speed. Fig. 8 shows a plot of V versus γ^- according to (67). For comparison we have also plotted the $V - \gamma^-$ relation $(14)_2$ for the shock wave in Problem 1. The two curves fall on top of each other, (the maximum relative difference between them in the range considered being approximately 0.15%), and therefore for clarity, we have shifted the curve corresponding to the shock (solid) by 0.1 units vertically. It follows that the strain and particle speed behind the DSW in Problem 3 is essentially identical to the strain and particle speed behind the shock in Problem 1. Recall from the discussion surrounding Fig. 4 that we previously made a similar observation between Problems 2 and 1.

In view of $\gamma^+ = 0, v^+ = 0$ and $(64)_2$, Eq. (62) reduces to

$$v_*(x,t) = v_*(m) = -(\beta_0^2/c_0^2)(c_{\text{soliton}} - c)^2(2c_{\text{soliton}} + c). \tag{69}$$

where

$$\frac{c(m)}{c_0} = \sqrt{1 + \frac{(1+m^2)\gamma^-}{3\beta_0^2}}. \tag{70}$$

Thus in summary, given the impact speed V, we find γ^- from (67), $m(x/t)$ from (58) and $v_*(x/t)$ from (69). The strain and particle speed fields within the DSW are then given by (59), (60) and (61) with $g^+ = 0, g^- = \gamma^-$. The fields are constant on either side of the DSW.

Fig. 9 shows a typical strain profile according to (58) and (59); the figure on the left plots $\gamma(x,t)$ versus t at fixed x, and that on the right shows the variation of $\gamma(x,t)$ with x at fixed t. Observe from $(38)_3$ and (43) that the first argument of the Jacobi Elliptic function in (59) can

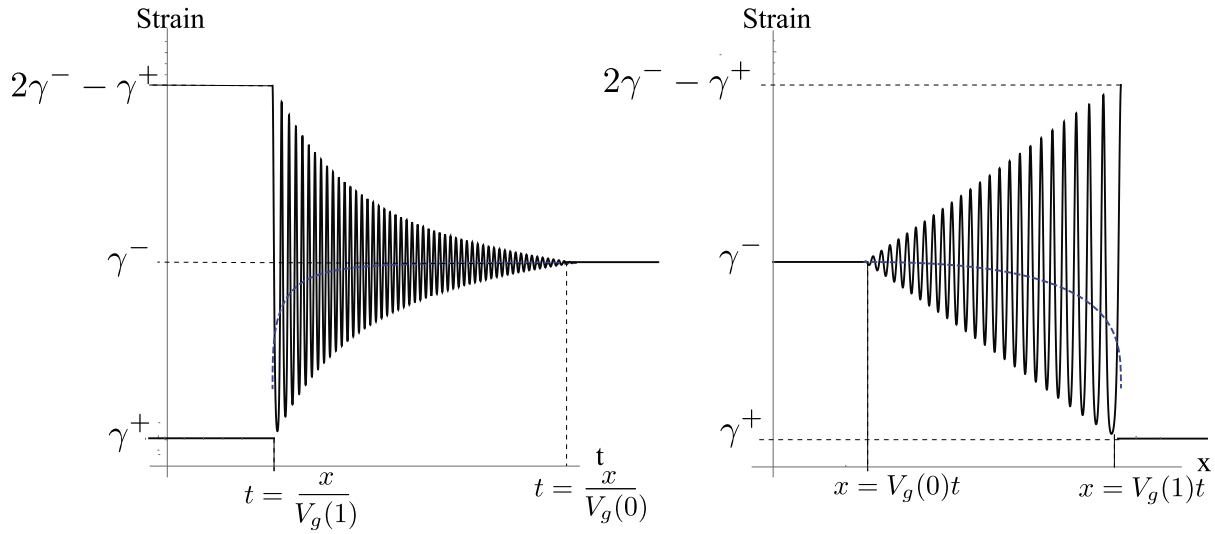

Fig. 9. Strain $\gamma(x,t)$ versus t at fixed x (left) and versus x at fixed t (right) according to (58) and (59). The leading and trailing edges travel at the respective speeds $V_g(1)$ and $V_g(0)$. The strain in front of the leading edge is γ^+, that behind the trailing edge is γ^-. The average strain given by (47), (58) are the dashed curves. In Problem 3 we have $\gamma^+ = 0$. While the figures have been drawn for $\eta_0 = 4/5$ and $h = 0.001$, see the comments surrounding (71).

be written as

$$\frac{K(m)}{\pi}\,\Phi = \sqrt{\frac{g^-}{6\beta_0^2}}\,\frac{x-ct}{h\sqrt{\eta_0}}. \tag{71}$$

Therefore if we nondimensionalize x by $h\sqrt{\eta_0}$ and t by $h\sqrt{\eta_0}/c_0$ in Fig. 9, the DSW strain profile will not depend on the parameters h and η_0. Note from (59) that the amplitude is independent of these parameters.

The approximate solution we have constructed is not appropriate at large values of the impact speed. The trailing edge of the DSW, $x = V_g(0)t$, must lie in the first quadrant of the x,t-plane. According to (44), this requires $\gamma^- < 3\beta_0^2$, which in turn by (67), demands that

$$\frac{V}{c_0\beta_0^2} \;<\; 2\big[3\sqrt{3}-2\sqrt{2}\big] \;\approx\; 4.735. \tag{72}$$

4.4. Oscillatory energy. Apparent dissipation

From $\sigma_x = \rho v_t$, $(33)_1$ and $(34)_2$ one can *derive* the local conservation law

$$\frac{\partial \mathcal{P}}{\partial x} = \frac{\partial \mathcal{E}}{\partial t}, \tag{73}$$

where

$$\mathcal{P} = \sigma v - \eta h^2 \gamma_x \gamma_t, \qquad \mathcal{E} = W - \frac{1}{2}\eta h^2 \gamma_x^2 + \frac{1}{2}\rho v^2. \tag{74}$$

Here $\mathcal{P}$ represents the power density (rate of working per unit length) and $\mathcal{E}$ is the *energy density* and so (73) is simply a statement of the elastic power identity ("conservation of energy"). In particular, the second term[10] in $\mathcal{E}$ can be identified with the energy associated with the strain-gradient term and the second term in $\mathcal{P}$ as the corresponding working of the associated "couple-stress".

According to the solution described schematically in Fig. 7, the strain and particle speed at each particle eventually settle down at the respective values γ^- and $v^- = -V$. Therefore at any point within or behind the DSW we set

$$\gamma_{\rm osc}(x,t) := \gamma(x,t) - \gamma^-, \qquad v_{\rm osc}(x,t) := v(x,t) - v^-. \tag{75}$$

Note that $\gamma_{\rm osc}$ and $v_{\rm osc}$ vanish behind the DSW, while within it, they represent the oscillatory parts of the strain and particle speed. We define the energy density associated with the oscillatory part of the motion to be[11]

$$\mathcal{E}_{\rm osc} := W(\gamma_{\rm osc}) - \frac{1}{2}\eta k^2 \big(\gamma'_{\rm osc}\big)^2 + \frac{1}{2}\rho v_{\rm osc}^2, \tag{76}$$

where $\gamma'_{\rm osc}$ is the derivative of $\gamma_{\rm osc}$ with respect to Φ. This is the oscillatory part of the energy density. The particles behind the DSW have zero oscillatory energy.

An alternative definition of the oscillatory strain and particle speed is

$$\gamma_{\rm osc}(x,t) := \gamma(x,t) - \big\langle \gamma \big\rangle, \qquad v_{\rm osc}(x,t) := v(x,t) - \big\langle v \big\rangle, \tag{77}$$

where, in the DSW, the average strain $\langle\gamma\rangle$ and average particle speed $\langle v\rangle$ are given by (47) and (50) specialized to Problem 3. The associated energy density is again given by (76).

Observe that the right-hand side of (76) can be expressed as a function of m and Φ and so we can write $\mathcal{E}_{\rm osc}(x,t) = \widehat{\mathcal{E}}_{\rm osc}(\Phi(x,t), m(x,t))$. We now average this energy density over the fast oscillations to get

$$\big\langle \mathcal{E}_{\rm osc} \big\rangle(m) = \frac{1}{2\pi}\int_0^{2\pi} \widehat{\mathcal{E}}_{\rm osc}(\Phi, m)\, d\Phi. \tag{78}$$

Finally, integrating $\langle \mathcal{E}_{\rm osc}\rangle(m)$ over the DSW tells us that the total oscillatory energy at time t

$$= \int_{V_g(0)t}^{V_g(1)t} \big\langle \mathcal{E}_{\rm osc} \big\rangle(m(x,t))\, dx = t\int_0^1 \big\langle \mathcal{E}_{\rm osc} \big\rangle(m) V'_g(m)\, dm, \tag{79}$$

where we have used $x = V_g(m)t$ in getting the second expression. The time *rate of increase of the total oscillatory energy* is therefore[12]

$$\mathcal{D} := \int_0^1 \big\langle \mathcal{E}_{\rm osc} \big\rangle(m) V'_g(m)\, dm. \tag{80}$$

[10] For energetic reasons one might therefore be inclined to let η have a negative value. However as noted previously since our goal is to mimic the discrete particle chain, we have taken η to be positive; see first paragraph of Section 4.

[11] Even though $\Phi(x,t) = (k(x,t)x - \omega(x,t)t)/h$ it still follows that $\partial\Phi/\partial x = k/h$ and $\partial\Phi/\partial t = -\omega/h$; see Section S5 of the electronic supplemental material.

[12] We also calculated this without averaging. In this case we integrated $\mathcal{E}_{\rm osc} := W(\gamma_{\rm osc}) - \frac{1}{2}\eta h^2\gamma_x^2 + \frac{1}{2}\rho v_{\rm osc}^2$ across the DSW to determine the total oscillatory energy $E_{\rm osc}(t)$. We plotted $E_{\rm osc}(t)$ versus t where the typical graph involved oscillations about a mean straight line. The slope of this straight line provided an estimate of the rate of increase of the total oscillatory energy, $\mathcal{D}$. The two methods of calculation gave essentially the same results.

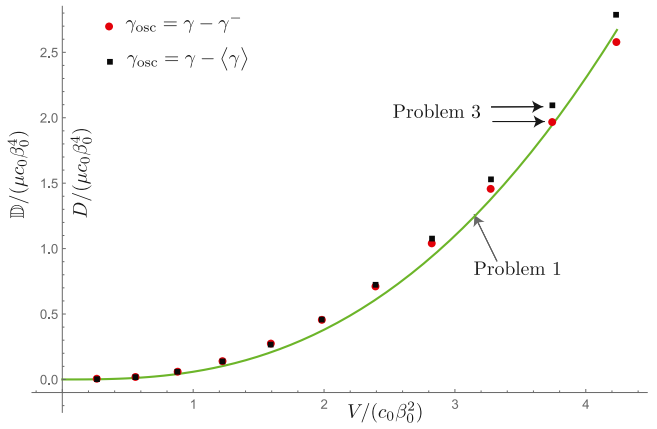

Fig. 10. Rate of increase of the total oscillatory energy $D/(\mu c_0\beta_0^4)$ in Problem 3 versus impact speed $V/(c_0\beta_0^2)$: the dots and squares in the figure correspond to the respective definitions (75) and (77) of the oscillatory strain and speed. When only one dot/square is visible, the other is right behind it. The dissipation rate $\mathbb{D}/(\mu c_0\beta_0^4)$ in Problem 1 is the solid curve.

At each impact speed V, we first determined $\gamma^-, \gamma(x,t)$ and $v(x,t)$ as described in the preceding sub-section. Then, for each definition (75) and (77) of the oscillatory strain and particle speed, we calculated $\mathcal{E}_{\rm osc}$ using (76); averaged it using (78); and finally calculated the rate of increase of the oscillatory energy, $\mathcal{D}$, using (80). Such calculations were carried out for several impact speeds (consistent with (72)) and the results are shown in Fig. 10. The dots and squares in the figure correspond to the respective definitions (75) and (77) of the oscillatory strain and speed. The solid curve is the dissipation rate in Problem 1 according to (16). These results will be discussed in Section 5.

Observe from (43) that k^2, the square of the wave number, is proportional to $1/\eta$. It therefore follows from (76) that the oscillatory energy density $\mathcal{E}_{\rm osc}$ does not depend on the value of the parameter η.

The average strain $\langle\gamma\rangle$ is smaller than γ^- in the interior of the DSW since $\langle\gamma\rangle$ decreases monotonically from γ^- at the trailing edge to zero at the leading edge. This presumably is why the associated rate of change of the oscillatory energy is slightly larger for (77) compared to (75) – the squares are above the dots.

5. Results and discussion

The aim of this paper was to understand the energy dissipated at a shock wave in a nonlinearly elastic bar (Problem 1) in terms of the energy in the oscillations in two related dissipationless, dispersive systems (Problems 2 and 3). The dissipation rate $\mathbb{D}$ in Problem 1 was calculated analytically, while the rate of change of the oscillatory energy D in Problem 2 was calculated numerically. An approximate analytical solution to Problem 3 was constructed using a calculation motivated by Whitham's modulation theory, and the rate of change of the oscillatory energy, D, was calculated by averaging over the fast oscillations of the modulated wave.

Our main result, the comparison of these quantities, is described graphically in Fig. 6 (Problems 1 and 2) and Fig. 10 (Problems 1 and 3).

The figures show that D is a good qualitative measure of $\mathbb{D}$. While the figures appear to suggest good quantitative agreement as well, this is only true for sufficiently large impact speeds. In Fig. 6, the relative difference $(D-\mathbb{D})/\mathbb{D}$ is less than 10% for impact speeds $V/(c_0\beta_0^2) \gtrapprox 1.75$, but the difference increases as the impact speed decreases, and exceeds 25% for $V/(c_0\beta_0^2) \lessapprox 1.0$. Similarly in Fig. 10, the relative difference $(D-\mathbb{D})/\mathbb{D}$ is less than 10% for impact speeds $V/(c_0\beta_0^2) \gtrapprox 2.75$, but the difference increases monotonically as the impact speed decreases, and exceeds 40% for $V/(c_0\beta_0^2) \lessapprox 1.0$.

We will discuss some possible reasons for this below. However, in addition to those reasons, as can be seen from the figures, the numerical values of D and $\mathbb{D}$ are very small at low impact speeds, and so small errors can have large quantitative effects in this range. In contrast, the values of D and $\mathbb{D}$ are larger for larger impact speeds where the agreement is better. Moreover, in determining the dissipation in Problem 2 we calculate the difference between two very small numbers — the work done at the boundary and the energy corresponding to the average strain and particle velocity behind the shock. This leads to inaccuracies.

In this paper we defined the oscillatory part of the strain γ_{osc} to be the difference between the strain and some base value of strain, where for the base strain we considered two alternatives, $\langle\gamma\rangle$ and γ^-. The oscillatory part of the particle speed, v_{osc}, was defined similarly. These seem to be fairly natural definitions. On the other hand it is less obvious as to how to quantify the "oscillatory energy" (the "energy in the oscillations"). While in this paper we describe the results for $E_{osc} := W(\gamma_{osc}) + \frac{1}{2}\rho v_{osc}^2$, we considered several alternatives: in particular, we considered the difference between various energies including the total energy in the DSW, the average of the total energy in the DSW, the energy associated with the average strain and speed in the DSW, the energy behind the DSW and so on. For example one alternative candidate we looked at was

$$\left\langle W(\gamma) + \frac{1}{2}\rho v^2 \right\rangle - \left(W\left(\langle\gamma\rangle\right) + \frac{1}{2}\rho \left\langle v \right\rangle^2 \right).$$

While the rate of change of oscillatory energy based on the alternatives we considered did not come anywhere near the dissipation rate of Problem 1 (e.g. see Figure S4 in Section S8), we were certainly not exhaustive in the alternatives we considered. More careful analysis of this is needed.

In our analysis of Problem 3, the steady periodic traveling wave for the strain involved 3 parameters g^+, g^- and m. However, in constructing the slowly modulated version of this solution we only allowed $m(x,t)$ to vary and took g^+ and g^- to be constants. Our motivation for this was based on the fact that in the impact problem of interest, the states on either side of the DSW had constant strains g^+ and g^-. But that does not necessitate g^+ and g^- to be constant within the DSW, and our assumption that g^+ and g^- are constant is not mathematically based. The natural next step would be to allow all of the parameters to vary and to determine them from a rigorous application of modulation theory by averaging the conservation laws in Section S7 of the electronic supplemental material. (While this may improve the comparison of the energetics of Problems 3 and 1, it will, of course, have no effect on that between Problems 2 and 1.)

Ultimately, no matter how good the comparison between the results, one would want to establish the relation between D and $\mathbb{D}$ mathematically, most probably in the dispersionless limits of Problems 2 and 3.

Declaration of competing interest

The authors declare that they have no known competing financial interests or personal relationships that could have appeared to influence the work reported in this paper.

Acknowledgments

The authors gratefully acknowledge valuable feedback from Phoebus Rosakis on a first draft of this manuscript. We also thank the anonymous reviewers for their careful reading of the manuscript and their insightful suggestions. RA thanks Zhantao Chen for his guidance with MATHEMATICA. PKP acknowledges partial support from a seed grant from the MRSEC at the University of Pennsylvania, United States, grant number NSF DMR-1720530.

Appendix A

In Problem 3, the constitutive equation for stress, $\sigma = \mu\gamma + \frac{1}{2}\alpha^2\gamma^2 + \eta h^2\gamma_{xx}$, had $\eta > 0$. This was motivated by the form of the continuum equation arrived at by Taylor expanding the discrete equations, e.g. Rosenau (1986). However this leads to instability if the wave length of a perturbation is too small (i.e. the wave number is too large). In this section we find the condition for linear stability, and confirm that the wave numbers within the DSW conform to it. Thus, if we limit attention to perturbations whose wave numbers are close to those in the DSW, linear stability is maintained.

Consider a point within the DSW where the strain and particle speed are $\overline{\gamma}$ and $\overline{v}$. To examine the stability of a steady uniform motion corresponding to this strain and particle speed, we substitute $\gamma = \overline{\gamma} + u_x, v = \overline{v} + u_t$ into the constitutive relation, and the result into the equation of motion. After linearization this leads to

$$\mu u_{xx} + \alpha^2\overline{\gamma}u_{xx} + \eta h^2 u_{xxxx} = \rho u_{tt}. \tag{81}$$

A steady periodic traveling wave solution of this linear equation has the form

$$u(x,t) = \exp i\Big(\frac{kx-\omega t}{h}\Big), \tag{82}$$

where k and ω are constants. Keep in mind that u is the perturbation and k is the wave number of the perturbation. Eqs. (81) and (82) lead to the dispersion relation

$$\omega^2/c_0^2 = (1+\overline{\gamma}/\beta_0^2)k^2 - \eta_0 k^4.$$

The right-hand side of this is negative when k is large, and this leads to imaginary values for ω, and the corresponding perturbation (82) becomes unbounded as $t \to \infty$. Thus linear stability requires the right-hand side of the dispersion relation to be nonnegative and so the wave number k must obey

$$1 + \overline{\gamma}/\beta_0^2 \geq \eta_0 k^2. \tag{83}$$

The inequality (83) is always violated if the wave number of the perturbation is sufficiently large. However, we now show that the wave numbers within the DSW satisfy (83). Locally, at each point within the DSW, the strain has the mean value $\langle\gamma\rangle$ and wave number $k(m)$ given by (43) and (46) respectively. Replacing $\overline{\gamma}$ and k in (83) by these expressions leads to

$$1 \geq \left[\frac{\pi^2/6}{K^2(m)} + 1 - m^2 - 2\frac{E(m)}{K(m)}\right]\frac{\gamma^-}{\beta_0^2}.$$

The term within the square brackets is negative and so this inequality holds automatically for all $\gamma^- > 0$.

Instead, if we replace $\overline{\gamma}$ by the smallest value of the strain, γ_{lower}, given by (S21) (and k by (43)), Eq. (83) yields

$$1 \geq \left[\frac{\pi^2/6}{K^2(m)} - 1 + m^2\right]\frac{\gamma^-}{\beta_0^2}.$$

The term in square brackets is positive and its maximum value is ≈ 0.148 and so this inequality holds provided $\gamma^-/\beta_0^2 \lessapprox 1/(0.148) = 6.75$. Recall from the line of text just above (72) that we restrict attention to strains $\gamma^- < 3\beta_0^2$.

Thus the wave numbers in the DSW lie within the range of linear stability given by (83). Therefore if the wave number of a perturbation is close the wave numbers within the DSW, we have stability against such a perturbation.

Appendix B. Supplementary data

Supplementary material related to this article can be found online at https://doi.org/10.1016/j.ijsolstr.2021.111371.

References

Abeyaratne, R., Knowles, J.K., 2006. Evolution of Phase Transitions: A Continuum Theory. Cambridge University Press.

Abeyaratne, R., Vedantam, S., 1999. Propagation of a front by kink motion. In: Argoul, P., Fremond, M., Nguyen, Q. (Eds.), 1997 IUTAM Symposium on Variations of Domains and Free Boundary Problems in Solid Mechanics. Kluwer, pp. 77–84.

Abeyaratne, R., Vedantam, S., 2003. A lattice-based model of the kinetics of twin boundary motion. J. Mech. Phys. Solids 51 (9), 1675–1700.

Atkinson, W., Cabrera, N., 1965. Motion of a Frenkel-Kontorowa dislocation in a one–dimensional crystal. Phys. Rev. 138 (3), A763 – 766.

Aubry, S., Proville, L., 2009. Pressure fronts in 1D damped nonlinear lattices. arXiv: Statistical Mechanics.

Byrd, P., Friedman, M., 1972. Handbook of Elliptic Integrals for Engineers and Scientists, second ed. Springer-Verlag.

Chin, R., 1975. Dispersion and Gibbs phenomenon associated with difference approximations to initial boundary-value problems for hyperbolic equations. J. Comput. Phys. 18, 233–247.

Courant, R., Friedrichs, K., 1978. Supersonic Flow and Shock Waves. Springer.

Dormand, J., Prince, P., 1980. A family of embedded Runge-Kutta formulae. J. Comput. Appl. Math. 6, 19–26.

Dreyer, W., Hermann, M., Mielke, A., 2005. Micro-macro transition in the atomic chain via Whitham's modulation equation. Nonlinearity 19, 471–500.

Dreyer, W., Hermann, M., 2008. Numerical experiments on the modulation theory for the nonlinear atomic chain. Physica D 237, 255–282.

El, G., Hoefer, M., 2016. Dispersive shock waves and modulation theory. Physica D 333, 11–65. http://dx.doi.org/10.1016/j.physd.2016.04.006.

Fermi, E., Pasta, P., Ulam, S., Tsingou, M., 1955. Studies of the nonlinear problems. http://dx.doi.org/10.2172/4376203, URL https://www.osti.gov/biblio/4376203.

Fornberg, B., Whitham, G., 1978. A numerical and theoretical study of certain nonlinear wave phenomena. Proc. R. Soc. Lond. Ser. A Math. Phys. Eng. Sci. 289, 373–403.

Frenkel, D., Smit, B., 2002. Understanding Molecular Simulation. Academic Press.

Friesecke, G., Pego, R., 1999. Solitary waves on FPU lattices: I. Qualitative properties, renormalization and continuum limit.. Nonlinearity 12, 1601–1627.

Gavrilyuk, S., Nkonga, B., Shyue, K.-M., Truskinovsky, L., 2020. Stationary shock-like transition fronts in dispersive systems. Nonlinearity 33, 5477–5509.

Giannoulis, J., Herrmann, M., Mielke, A., 2006. Continuum descriptions for the dynamics in discrete lattices: Derivation and justification. In: Mielke, A. (Ed.), Analysis, Modeling and Simulation of Multiscale Problems. Springer, Berlin, Heidelberg, pp. 435–466. http://dx.doi.org/10.1007/3-540-35657-6_16.

Giannoulis, J., Mielke, A., 2004. The nonlinear Schrödinger equation as a macroscopic limit for an oscillator chain with cubic nonlinearities. Nonlinearity 17, 551–565.

Giannoulis, J., Mielke, A., 2006. Dispersive evolution of pulses in oscillator chains with general interaction potentials. Discrete Contin. Dyn. Syst. Ser. B 3, 493–523.

Grava, T., Klein, C., 2007. Numerical solution of the small dispersion limit of Korteweg–de Vries and Whitham equations. Comm. Pure Appl. Math. LX, 1623–1664.

Gurevich, A., Pitaevskii, L., 1973. Nonstationary structure of a collisionless shock wave. Zh. Eksp. Teor. Fiz. 65 (2), 590–604, in Russian.

Gurevich, A., Pitaevskii, L., 1974. Nonstationary structure of a collisionless shock wave. Sov. J. Exper. Theor. Phys. 38 (2), 291–297.

Hauch, J., Marder, M., 1998. Energy balance in dynamic fracture, investigated by a potential drop technique. Int. J. Fract. 90, 133–151. http://dx.doi.org/10.1023/A:1007491318198.

Hermann, M., 2012. Oscillatory waves in discrete scalar conservation laws. Math. Models Methods Appl. Sci. 22 (1), http://dx.doi.org/10.1142/S021820251200585X.

Hoefer, M., Ablowitz, M., Coddington, I., Cornell, E., Engels, P., Schweikhard, V., 2006. Dispersive and classical shock waves in bose-Einstein condensates and gas dynamics. Phys. Rev. A 74 (2), 023623.

Kamchatnov, A.M., 2000. Nonlinear Periodic Waves and their Modulations: An Introductory Course. World Scientific Publishing.

Kresse, O., Truskinovsky, L., 2003. Mobility of lattice defects: discrete and continuum approaches. J. Mech. Phys. Solids 51, 1305–1332.

Lax, P., Levermore, C., 1983a. The small dispersion limit of the Korteweg-de Vries equation: part 1. Comm. Pure Appl. Math. 36 (3), 253–290.

Lax, P., Levermore, C., 1983b. The small dispersion limit of the Korteweg-de Vries equation: part 2. Comm. Pure Appl. Math. 36 (5), 571–593.

Lax, P., Levermore, C., 1983c. The small dispersion limit of the Korteweg-de Vries equation: part 3. Comm. Pure Appl. Math. 36 (6), 809–830.

Nguyen, L., 1987. Whitham Modulation Theory and Direct Methods for Nonlinear Dispersive Waves. (Ph.D. thesis). Ruhr-Universität Bochum, URL https://hss-opus.ub.ruhr-uni-bochum.de/opus4/frontdoor/deliver/index/docId/5049/file/diss.pdf.

Nguyen, L., Smyth, N., 2021. Dispersive shock waves for the Boussinesq Benjamin–Ono equation. Stud. Appl. Math. 147 (1), 32–59.

Oleinik, O., 1959. Uniqueness and stability of the generalized solution of the Cauchy problem for a quasilinear equation. Uspekhi Matematicheskii Nauk (N.S.) 14, 165–170, in Russian.

Olver, F., Olde Daalhuis, A., Lozier, D., Schneider, B., Boisvert, R., Clark, C., Miller, B., Saunders, B., Cohl, H., McClain, M.e. (Eds.), 2021. NIST Digital Library of Mathematical Functions. URL http://dlmf.nist.gov/ (Acessed 15 June 2021).

Puglisi, G., Truskinovsky, L., 2000. Mechanics of a discrete chain with bi-stable elements. J. Mech. Phys. Solids 48, 1–27.
Purohit, P., Bhattacharya, K., 2003. Dynamics of strings made of phase transforming materials. J. Mech. Phys. Solids 51, 393–424.
Ratliff, D., Bridges, T., 2016. Whitham modulation equations, coalescing characteristics, and dispersive Boussinesq dynamics. Physica D 333, 107–116.
Rosenau, P., 1986. Dynamics of nonlinear mass-spring chains near the continuum limit. Phys. Lett. A 118, 222–227.
Shampine, L., Reichelt, M., 1997. The MATLAB suite. SIAM J. Sci. Comput. 18, 1–22.
Sharma, B.L., 2005. The kinetic relation of a Peierls dislocation in a higher-gradient dispersive continuum. (Ph.D. thesis). Cornell University.
Slepyan, L., Cherkaev, A., Cherkaev, E., 2005. Transition waves in bistable structures. II. Analytical solution: wave speed and energy dissipation. J. Mech. Phys. Solids 53, 407–436.
Synge, J., 1973. Linked harmonic oscillators. SIAM J. Appl. Math. 25 (3), 335–345.
Truskinovsky, L., 1982. Equilibrium phase boundaries. Sov. Phys. Dokl. 27, 551–553.
Truskinovsky, L., Vainchtein, A., 2005. Kinetics of martensitic phase transitions: lattice model. SIAM J. Appl. Math. 66, 533–553.
Venakides, S., 1985. The zero-dispersion limit of the Korteweg-de Vries equation with non-trivial reflection coefficient. Comm. Pure Appl. Math. 38, 125–155.
Whitham, G., 1965a. A general approach to linear and non-linear dispersive waves using a Lagrangian. J. Fluid Mech. 22 (2), 273–283.
Whitham, G., 1965b. Non-linear dispersive waves. Proc. Royal Soc. Lond. Series A. Math. Phys. Sci. 283 (2), 238–261.
Whitham, G., 1967. Non-linear dispersion of water waves. J. Fluid Mech. 27 (2), 399–412.
Whitham, G., 1970. Two-timing, variational principles and waves. J. Fluid Mech. 44 (2), 373–395.
Whitham, G., 1974. Linear and Nonlinear Waves. John Wiley.
Zhao, Q., Purohit, P., 2016. (Adiabatic) phase boundaries in a bistable chain with twist and stretch. J. Mech. Phys. Solids 92, 176–194.